

# Lifshitz theory of atom-wall interaction with applications to quantum reflection

V. B. Bezerra,<sup>1</sup> G. L. Klimchitskaya,<sup>2,\*</sup> V. M. Mostepanenko,<sup>2,†</sup> and C. Romero<sup>1</sup>

<sup>1</sup>*Department of Physics, Federal University of Paraíba,*

*C.P.5008, CEP 58059-970, João Pessoa, Pb-Brazil*

<sup>2</sup>*Center of Theoretical Studies and Institute for Theoretical Physics,*

*Leipzig University, Postfach 100920, D-04009, Leipzig, Germany*

## Abstract

The Casimir-Polder interaction of an atom with a metallic wall is investigated in the framework of the Lifshitz theory. It is demonstrated that in some temperature (separation) region the Casimir-Polder entropy takes negative values and goes to zero when the temperature vanishes. This result is obtained both for an ideal metal wall and for real metal walls. Simple analytical representations for the Casimir-Polder free energy and force are also obtained. These results are used to make a comparison between the phenomenological potential used in the theoretical description of quantum reflection and exact atom-wall interaction energy, as given by the Lifshitz theory. Computations are performed for the atom of metastable He\* interacting with metal (Au) and dielectric (Si) walls. It is shown that the relative differences between the exact and phenomenological interaction energies are smaller in the case of a metallic wall. This is explained by the effect of negative entropy which occurs only for a metal wall. More accurate atom-wall interaction energies computed here can be used for the interpretation of measurement data in the experiments on quantum reflection.

PACS numbers: 34.35.+a, 12.20.Ds, 34.50.Cx

---

\* on leave from North-West Technical University, St.Petersburg, Russia

† on leave from Noncommercial Partnership “Scientific Instruments”, Moscow, Russia

## I. INTRODUCTION

Atom-wall interaction, which is a special case of dispersion interactions caused by quantum fluctuations, plays an important role in different physical, chemical and biological phenomena [1]. At short separations from several angstroms to a few nanometers the interaction of an atom with a wall is described by the nonretarded van der Waals potential of the form  $V_3 = -C_3/a^3$  [2]. At separations of about  $1\ \mu\text{m}$  the interaction between an atom and a wall is of relativistic character and is described by the Casimir-Polder potential  $V_4 = -C_4/a^4$  [3]. The Lifshitz theory [4, 5] provides a complete description of atom-wall interaction including the transition region from the nonrelativistic to relativistic regime. It also predicts that at separations larger than a few micrometers thermal effects become dominating. The Lifshitz theory takes into account realistic properties of an atom and of a wall material. In so doing atom is described by the dynamic polarizability as a function of frequency and wall by the frequency-dependent dielectric permittivity. Over a period of years many experiments were performed on measuring atom-wall interaction in different separation regions. From the theoretical side, more accurate expressions for the atom-wall interaction energy were obtained (see Refs. [6, 7, 8] for the literature on the subject and calculational results).

On the modern stage of experimental research of atom-wall interaction, the magnitude and the distance dependence of the Casimir-Polder force were confirmed in Ref. [9] when studying the deflection of ground-state Na atoms passing through a micron-sized parallel plate cavity. The experimental data were compared with the theoretical position-dependent potential for an atom between parallel ideal metal plates [10, 11]. Of special interest are situations when the wave nature of atom becomes dominant with respect to its classical behavior as a particle. Such a pure quantum effect is what is called *quantum reflection*, i.e., a process in which a particle moving through a classically allowed region is reflected by a potential without reaching a classical turning point. This is in fact a reflection of an ultracold atom under the influence of an *attractive* atom-wall interaction or, in other words, the above-barrier reflection. The phenomenon of quantum reflection has become observable due to the success in the production of ultracold atoms. First it was demonstrated with liquid surfaces [12, 13, 14, 15] and then with Si, glass [16],  $\alpha$ -quartz crystal [17] and Cu surfaces [18]. It was shown [19] that quantum reflection is particularly sensitive to details of the atom-surface interaction energy. On the other hand, low-energy scattering from asymptotic

power law potentials on metallic surfaces was examined in Ref. [20].

For theoretical calculation of the reflection amplitude, a simple phenomenological atom-wall interaction potential is commonly used [17, 21, 22], which is an interpolation between the nonretarded van der Waals potential  $V_3$  and the Casimir-Polder potential  $V_4$ . The comparison of computational results with the measurement data for the reflection amplitudes allows one to estimate the parameters of the phenomenological potential. However, the increasing precision of the measurements requests comparison with the more accurate atom-wall interaction potentials obtained from the Lifshitz theory and taking into account realistic properties of the atom and the material of the wall.

In this paper we investigate the characteristic properties of the interaction of atoms with metallic walls in the framework of the Lifshitz theory. We start with the case of an ideal metal wall and obtain the analytical expressions for the Casimir-Polder free energy and force in different separation and temperature regions. The delicate point that in the limit of short separation distances the interaction energy depends on the velocity of light is discussed. The asymptotic behavior of the Casimir-Polder entropy at low temperatures (short separations), which is typical for any model of the metal, is investigated. Negative values of the entropy arising within some region of separations are linked to a similar situation in the configuration of metal-dielectric [23, 24, 25]. Then, we summarize the calculation results for an atom interacting with a wall made of real metal and obtain simple analytical expressions for the Casimir-Polder interaction energy and force applicable to moderate atom-wall separations. Special attention is paid to the asymptotic behavior of the Casimir-Polder entropy at low temperatures. It is shown that the entropy goes to zero when the temperature vanishes, in accordance with the Nernst heat theorem. (Recall that violation of Nernst's theorem occurs for two parallel plates described by the Drude model with vanishing relaxation parameter when temperature vanishes [26]; this situation was debated in the literature, see, e.g., Refs. [27, 28, 29, 30].) However, we show that at low temperatures the Casimir entropy of the atom-wall interaction for real metal wall approaches zero from the negative values like this occurs for an ideal metal wall. Finally we compare the phenomenological potentials used in the calculation of reflection amplitudes in quantum reflection with the accurate results of numerical calculations using the Lifshitz formula. Both the cases of metallic (Au) and dielectric (Si) walls interacting with an atom of metastable  $\text{He}^*$  are considered. It is shown that the maximum deviation between the phenomenological and accurate results achieves

12.5% for Si at a separation  $a = 300$  nm and 10.5% for Au at  $a = 400$  nm. Increasing the separation, larger deviations between the accurate and phenomenological potential occur, especially for dielectric walls. It is shown that the effect of negative Casimir-Polder entropy, discovered in this paper in the configuration of an atom near a metal wall, makes the deviation between the accurate and phenomenological potentials smaller. Thus, with increasing experimental precision the use of more accurate expressions for the interaction energy in the calculation of reflection amplitudes may become preferable.

The paper is organized as follows. In Sec. II we briefly summarize the main results and notations used in the subsequent sections. Section III contains consideration of an atom near an ideal metal wall. In Sec. IV simple analytical expressions for the case of real metal wall are obtained. In Sec. V the low-temperature asymptotic behavior of the Casimir-Polder entropy is discussed. Section VI is devoted to the comparison between the phenomenological interaction energy commonly used to describe quantum reflection and a more accurate one obtained from the Lifshitz theory. Our conclusions and discussion are contained in Sec. VII.

## II. LIFSHITZ FORMULAS FOR AN ATOM NEAR A WALL

In accordance with the Lifshitz theory, the free energy of an atom-wall interaction for a wall at temperature  $T$  in thermal equilibrium with environment is given by

$$\mathcal{F}(a, T) = -k_B T \sum_{l=0}^{\infty}{}' \alpha(i\xi_l) \int_0^{\infty} k_{\perp} dk_{\perp} q_l e^{-2aq_l} \quad (1)$$

$$\times \left\{ 2r_{\text{TM}}(i\xi_l, k_{\perp}) - \frac{\xi_l^2}{q_l^2 c^2} [r_{\text{TM}}(i\xi_l, k_{\perp}) + r_{\text{TE}}(i\xi_l, k_{\perp})] \right\}.$$

Here,  $a$  is the separation distance between an atom and a wall,  $\alpha(\omega)$  is the atomic dynamic polarizability,  $\xi_l = 2\pi k_B T l / \hbar$  with  $l = 0, 1, 2, \dots$  are the Matsubara frequencies,  $k_B$  is the Boltzmann constant,  $k_{\perp}$  is the projection of the wave vector on the plane of a wall (i.e., perpendicular to the  $z$  direction), prime near the summation sign means that a multiple  $1/2$  is added to the term with  $l = 0$ , and  $q_l^2 = k_{\perp}^2 + \xi_l^2/c^2$ . The reflection coefficients for two independent polarizations of the electromagnetic field, transverse magnetic (TM) and transverse electric (TE), are given by

$$r_{\text{TM}}(i\xi_l, k_{\perp}) = \frac{\varepsilon_l q_l - k_l}{\varepsilon_l q_l + k_l}, \quad r_{\text{TE}}(i\xi_l, k_{\perp}) = \frac{q_l - k_l}{q_l + k_l}, \quad (2)$$

where  $k_l^2 = k_\perp^2 + \varepsilon_l \xi_l^2 / c^2$  and  $\varepsilon_l = \varepsilon(i\xi_l)$  is the frequency-dependent dielectric permittivity of the wall material calculated at the imaginary Matsubara frequencies.

From Eq. (1), we obtain the Lifshitz-type formula for the Casimir-Polder force acting on an atom near a wall:

$$\begin{aligned}
F(a, T) &= -\frac{\partial \mathcal{F}(a, T)}{\partial a} \\
&= -2k_B T \sum_{l=0}^{\infty}{}' \alpha(i\xi_l) \int_0^\infty k_\perp dk_\perp q_l^2 e^{-2aq_l} \\
&\times \left\{ 2r_{\text{TM}}(i\xi_l, k_\perp) - \frac{\xi_l^2}{q_l^2 c^2} [r_{\text{TM}}(i\xi_l, k_\perp) + r_{\text{TE}}(i\xi_l, k_\perp)] \right\}.
\end{aligned} \tag{3}$$

The interesting characteristic feature of Eqs. (1) and (3) describing atom-wall interaction is that the transverse electric reflection coefficient at zero frequency,  $r_{\text{TE}}(0, k_\perp)$ , does not contribute to the result as it is multiplied by the factor  $\xi_0^2 = 0$ . Because of this, in the case of metal wall the obtained values of the free energy and force do not depend on the model used for the metal. However, in the case of a dielectric wall, the results obtained depend on the transverse magnetic reflection coefficient at zero frequency,  $r_{\text{TM}}(0, k_\perp)$ . This can be used as a test for the model of the dielectric permittivity of the wall material [24, 25, 31, 32, 33, 34, 35].

Below we perform some analytical calculations of the van der Waals and Casimir-Polder interactions. Also numerical computations are performed for metastable He\* atoms and walls made of different materials. For both these purposes it is useful to express Eqs. (1) and (3) in terms of the dimensionless variables

$$\begin{aligned}
y &= 2q_l a, & \zeta_l &= \frac{\xi_l}{\omega_c} = \tau l, \\
\tau &= 4\pi \frac{k_B a T}{\hbar c} = 2\pi \frac{T}{T_{\text{eff}}},
\end{aligned} \tag{4}$$

where  $\omega_c \equiv c/(2a)$  is the so-called *characteristic frequency* and  $T_{\text{eff}} = \hbar\omega_c/k_B$  is the *characteristic temperature*. Then, the Casimir-Polder free energy for an atom near a wall is given by

$$\begin{aligned}
\mathcal{F}(a, T) &= -\frac{k_B T}{8a^3} \sum_{l=0}^{\infty}{}' \alpha(i\zeta_l \omega_c) \int_{\zeta_l}^{\infty} dy e^{-y} \\
&\times \left\{ 2y^2 r_{\text{TM}}(i\zeta_l, y) - \zeta_l^2 [r_{\text{TM}}(i\zeta_l, y) + r_{\text{TE}}(i\zeta_l, y)] \right\}.
\end{aligned} \tag{5}$$

The reflection coefficients are expressed in these variables in the following way:

$$\begin{aligned} r_{\text{TM}}(i\zeta, y) &= \frac{\varepsilon y - \sqrt{y^2 + \zeta^2(\varepsilon - 1)}}{\varepsilon y + \sqrt{y^2 + \zeta^2(\varepsilon - 1)}}, \\ r_{\text{TE}}(i\zeta, y) &= \frac{y - \sqrt{y^2 + \zeta^2(\varepsilon - 1)}}{y + \sqrt{y^2 + \zeta^2(\varepsilon - 1)}}, \quad \varepsilon \equiv \varepsilon(i\omega_c \zeta). \end{aligned} \quad (6)$$

The respective expression for the Casimir force acting on an atom is

$$\begin{aligned} F(a, T) &= -\frac{k_B T}{8a^4} \sum_{l=0}^{\infty} \alpha(i\zeta_l \omega_c) \int_{\zeta_l}^{\infty} dy y e^{-y} \\ &\times \{2y^2 r_{\text{TM}}(i\zeta_l, y) - \zeta_l^2 [r_{\text{TM}}(i\zeta_l, y) + r_{\text{TE}}(i\zeta_l, y)]\}. \end{aligned} \quad (7)$$

Note that here we consider atoms in the ground state and assume that thermal radiation is not so strong to excite electrons to higher states. The case of excited atoms is discussed in Ref. [36]. The possible impact of virtual photon absorption on the Casimir-Polder force was considered in Ref. [37].

The Casimir-Polder free energy, as given in Eq. (5), can be represented in the form

$$\mathcal{F}(a, T) = \mathcal{E}(a, T) + \Delta\mathcal{F}(a, T). \quad (8)$$

Here, the quantities  $\mathcal{E}(a, T)$  and  $\Delta\mathcal{F}(a, T)$  are obtained from Eq. (5) by the application of the Abel-Plana formula [38, 39]

$$\sum_{n=0}^{\infty} {}' F(n) = \int_0^{\infty} F(t) dt + i \int_0^{\infty} \frac{dt}{e^{2\pi t} - 1} [F(it) - F(-it)]. \quad (9)$$

They are given by

$$\begin{aligned} \mathcal{E}(a, T) &= \frac{\hbar c}{32\pi a^4} \int_0^{\infty} d\zeta \int_{\zeta}^{\infty} dy h(\zeta, y), \\ h(\zeta, y) &= -\alpha(i\omega_c \zeta) e^{-y} \{2y^2 r_{\text{TM}}(i\zeta, y) \\ &\quad - \zeta^2 [r_{\text{TM}}(i\zeta, y) + r_{\text{TE}}(i\zeta, y)]\}, \\ \Delta\mathcal{F}(a, T) &= \frac{i\hbar c \tau}{32\pi a^4} \int_0^{\infty} dt \frac{H(it\tau) - H(-it\tau)}{e^{2\pi t} - 1}, \\ H(x) &\equiv \int_x^{\infty} dy h(x, y). \end{aligned} \quad (10)$$

For the temperature-independent permittivities one gets  $\mathcal{E}(a, T) = E(a)$ , where  $E(a)$  is the Casimir-Polder energy at zero temperature, and  $\Delta\mathcal{F}(a, T) = \Delta_T \mathcal{F}(a, T)$ , the thermal correction to it.

Equations (1) and (3) present the Casimir-Polder energy and force at any separation between an atom and a wall. In the nonrelativistic limit (short separations if compared with the characteristic absorption wavelength of plate material) summation in these equations can be replaced by integration along continuous frequencies. At such short separations the velocity of light  $c$  can effectively be put equal to infinity. Then, the Casimir-Polder (van der Waals) atom-wall interaction energy is given by

$$\begin{aligned}
E(a) &= -\frac{\hbar}{2\pi} \int_0^\infty d\xi \alpha(i\xi) \int_0^\infty k_\perp dk_\perp \sqrt{k_\perp^2 + \frac{\xi^2}{c^2}} \\
&\times e^{-2a\sqrt{k_\perp^2 + \frac{\xi^2}{c^2}}} \left\{ 2r_{\text{TM}}(i\xi, k_\perp) \right. \\
&\quad \left. - \frac{\xi^2}{c^2 k_\perp^2 + \xi^2} [r_{\text{TM}}(i\xi, k_\perp) + r_{\text{TE}}(i\xi, k_\perp)] \right\} \\
&\approx -\frac{\hbar}{\pi} \int_0^\infty d\xi \alpha(i\xi) \int_0^\infty k_\perp^2 dk_\perp e^{-2ak_\perp} r_{\text{TM}}(i\xi, k_\perp).
\end{aligned} \tag{11}$$

In the nonrelativistic limit, from Eq. (2) one obtains

$$r_{\text{TM}}(i\xi, k_\perp) \approx \frac{\varepsilon(i\xi) - 1}{\varepsilon(i\xi) + 1}. \tag{12}$$

Substituting this result into Eq. (11) one arrives at the van der Waals energy for atom-wall interaction

$$V_3 = E(a) = -\frac{C_3}{a^3}, \quad C_3 = \frac{\hbar}{4\pi} \int_0^\infty d\xi \alpha(i\xi) \frac{\varepsilon(i\xi) - 1}{\varepsilon(i\xi) + 1}. \tag{13}$$

In the case of the relativistic limit of atom-wall interaction, it is considered below separately for ideal and real metals.

### III. ATOM NEAR AN IDEAL METAL PLANE

The configuration of an atom near metallic wall suggests some interesting and unexpected features connected with the behavior of the Casimir-Polder entropy at low temperature. This can be observed already in the simplest case of an atom interacting with an ideal metal plane. The Casimir-Polder free energy of atom-wall interaction is given by Eq. (1). From substitution of the reflection coefficients for an ideal metal plane,

$$r_{\text{TM}}(i\xi_l, k_\perp) = 1, \quad r_{\text{TE}}(i\xi_l, k_\perp) = -1, \tag{14}$$

one obtains

$$\mathcal{F}(a, T) = -2k_B T \sum_{l=0}^{\infty} \alpha(i\xi_l) \int_0^\infty k_\perp dk_\perp q_l e^{-2aq_l}. \tag{15}$$

In the region of short and moderate separation distances between an atom and a metal plane, where the thermal effects can be neglected, the free energy is approximately equal to the energy. The latter can be obtained from Eqs. (11) and (14)

$$E(a) = -\frac{\hbar}{\pi} \int_0^\infty d\xi \alpha(i\xi) \int_0^\infty k_\perp dk_\perp q e^{-2aq}. \quad (16)$$

Introducing the dimensionless variables  $y = 2aq$ ,  $\zeta = \xi/\omega_c$  and integrating with respect to  $y$ , we can rearrange this equation to the form

$$E(a) = -\frac{\hbar c}{16\pi a^4} \int_0^\infty d\zeta \alpha(i\omega_c \zeta) (\zeta^2 + 2\zeta + 2) e^{-\zeta}. \quad (17)$$

If we consider moderate separations from about  $1 \mu\text{m}$  to  $3 \mu\text{m}$  only, the approximation of a static atomic polarizability,  $\alpha(i\omega_c \zeta) \approx \alpha(0)$ , works well. In this case, Eq. (17) leads to

$$V_4 = E(a) \equiv E_{\text{CP}}(a) = -\frac{C_4}{a^4} = -\frac{3\hbar c}{8\pi a^4} \alpha(0). \quad (18)$$

This result was first obtained by Casimir and Polder [3] and corresponds to the relativistic atom-wall interaction potential.

At all separations larger than 50–70 nm the single-oscillator model for the dynamic atomic polarizability leads to less than 1% deviations from the calculational results using highly accurate atomic polarizabilities [8]. The single-oscillator model presents  $\alpha(i\xi)$  in the form

$$\alpha(i\xi) = \frac{\alpha(0)}{1 + \frac{\xi^2}{\omega_0^2}} = \frac{\alpha(0)}{1 + \frac{\omega_c^2}{\omega_0^2} \zeta^2} \equiv \alpha(i\omega_c \zeta). \quad (19)$$

Here,  $\omega_0$  is the characteristic absorption frequency for the atom under consideration. We perform calculation under the assumption that  $\beta_A \equiv \omega_c/\omega_0 = \lambda_0/(4\pi a) \gg 1$ , where  $\lambda_0 = 2\pi c/\omega_0$  is the characteristic absorption wavelength of an atom. This assumption is satisfied at atom-plane separations  $a \ll \lambda_0$ . We have once more introduced the new variables in Eq. (16), but changed the order of integrations in  $\zeta$  and  $y$  rather than first integrate with respect to  $y$  as was done previously. The result is

$$E(a) = -\frac{\hbar c}{16\pi a^4} \int_0^\infty y^2 dy e^{-y} \int_0^y d\zeta \alpha(i\omega_c \zeta). \quad (20)$$

Substituting Eq. (19) into Eq. (20) and integrating in  $\zeta$ , we get

$$E(a) = -\frac{\hbar c}{16\pi a^4} \alpha(0) \frac{1}{\beta_A} \int_0^\infty y^2 dy e^{-y} \arctan(\beta_A y). \quad (21)$$



Taking into account that  $\beta_A \gg 1$ , it is possible to replace  $\arctan(\beta_A y)$  with  $\pi/2$  without loss of accuracy. This leads to

$$E(a) = -\frac{\hbar c}{4\lambda_0 a^3} \alpha(0). \quad (22)$$

Note that although in Eq. (22) the same distance dependence appears (inverse third power of separation), as in the nonrelativistic limit in Eq. (13), it is quite different in nature. Particularly Eq. (13) does not contain the velocity of light, as is appropriate for the nonrelativistic limit, whereas Eq. (22) does. In fact, the nonrelativistic limit cannot be achieved for an ideal metal wall, because the characteristic absorption wavelength of an ideal metal is zero. The dependence of the Casimir-Polder energy at short separation distances in Eq. (22) on the velocity of light should be considered as an indication that at these separations the approximation of ideal metal is not applicable.

Now, we consider any separation distance larger than  $1 \mu\text{m}$  including those larger than  $3 \mu\text{m}$ . Here, one can use the static atomic polarizability, but should take thermal effects into account. Introducing the dimensionless variables (4) we rearrange the free energy given by Eq. (15) into the form

$$\mathcal{F}(a, T) = -\frac{k_B T}{4a^3} \alpha(0) \sum_{l=0}^{\infty} \int_{\zeta_l}^{\infty} y^2 dy e^{-y}. \quad (23)$$

After performing the integration and summation one obtains

$$\mathcal{F}(a, T) = E_{\text{CP}}(a) \eta(a, T), \quad (24)$$

where the Casimir-Polder energy is given in Eq. (18) and the correction factor is

$$\eta(a, T) = \frac{\tau}{6} \left[ 1 + \frac{2}{e^\tau - 1} + \frac{2\tau e^\tau}{(e^\tau - 1)^2} + \frac{\tau^2 e^\tau (e^\tau + 1)}{(e^\tau - 1)^3} \right]. \quad (25)$$

Note that the parameter  $\tau$ , defined in Eq. (4), is linear in separation and temperature. The asymptotic behavior of the correction factor (25) at low temperature is given by

$$\eta(a, T) = 1 - \frac{\tau^4}{2160} + \frac{\tau^6}{15120} - \frac{\tau^8}{241920} + O(\tau^{10}). \quad (26)$$

The Casimir-Polder force between an atom and an ideal metal plane can also be presented in a form similar to Eq. (24). For this purpose one can use Eq. (7) with the reflection coefficients (14) or calculate the negative derivative with respect to  $a$  from both sides of Eq. (24). The result is

$$F(a, T) = F_{\text{CP}}(a) \kappa(a, T), \quad F_{\text{CP}}(a) = -\frac{3\hbar c}{2\pi a^5} \alpha(0). \quad (27)$$

The correction factor to the Casimir-Polder force  $F_{\text{CP}}(a)$  can be represented as

$$\kappa(a, T) = \frac{3}{4}\eta(a, T) + \frac{\tau^4 e^\tau (e^{2\tau} + 4e^\tau + 1)}{24(e^\tau - 1)^4}. \quad (28)$$

The asymptotic behavior of this correction factor at low temperature is given by

$$\kappa(a, T) = 1 - \frac{\tau^6}{30240} - \frac{\tau^8}{241920} + O(\tau^{10}). \quad (29)$$

It is interesting that representations like (24) and (26) for the free energy or (27) and (29) for the force of atom-wall interaction can be obtained directly from the Lifshitz formulas describing the Casimir interaction between metallic and dielectric plates when the dielectric plate is dilute [23, 24, 25].

Now, we are in a position to find the entropy of the Casimir-Polder interaction. Calculating the negative derivative of Eq. (24) with respect to the temperature, we get the expression

$$S(a, T) = \frac{3k_B}{2a^3}\alpha(0)\sigma(a, T), \quad (30)$$

where

$$\sigma(a, T) = \frac{1}{\tau}\eta(a, T) - \frac{\tau^3 e^\tau (e^{2\tau} + 4e^\tau + 1)}{6(e^\tau - 1)^4}. \quad (31)$$

It can easily be seen that the asymptotic expansion of the entropy factor,  $\sigma$ , at low temperature is given by

$$\sigma(a, T) = -\frac{\tau^3}{540} + \frac{\tau^5}{2520} + O(\tau^7). \quad (32)$$

Thus, the Casimir-Polder entropy goes to zero when temperature vanishes in accordance with the Nernst heat theorem. Note, however, that at low temperatures (small  $\tau$ ) the entropy (30) takes negative values. In Fig. 1 we plot the entropy factor  $\sigma$  from Eq. (30) in the configuration of an atom near an ideal metal plane as a function of  $\tau$ . As is seen in Fig. 1, the Casimir-Polder entropy is negative for  $0 < \tau < 3$  and positive for larger  $\tau$ . This is in accordance with the respective results for the configuration of metal and dielectric plates [23, 24, 25]. Keeping in mind that the Lifshitz formula for an atom near a metal plate is obtained from the formula describing the two parallel plates one of which being metallic and the other a dilute dielectric, the similarity obtained in the behavior of entropy appears quite natural.

In the high temperature limit  $T \gg T_{\text{eff}}$ , only the zero-frequency term in Eq. (23) determines the total result, whereas all terms with  $l \geq 1$  are exponentially small. In this case

Eq. (23) leads to

$$\mathcal{F}(a, T) = -\frac{k_B T}{4a^3} \alpha(0). \quad (33)$$

This is the classical limit [40, 41] of the Casimir-Polder free energy because the right-hand side of Eq. (33) does not depend on  $\hbar$ . In this situation, the respective expressions for the Casimir-Polder entropy and force are given by

$$S(a, T) = -\frac{k_B}{4a^3} \alpha(0), \quad F(a, T) = -\frac{3k_B T}{4a^4} \alpha(0). \quad (34)$$

#### IV. ATOM NEAR A REAL METAL PLATE

Here, we consider a metal plate made of Au described by the plasma model

$$\varepsilon(\omega) = 1 - \frac{\omega_p^2}{\omega^2} \quad (35)$$

with the plasma frequency  $\omega_p = 9.0$  eV. This allows rather precise results at separation distances larger than the plasma wavelength  $\lambda_p = 137$  nm. At these separations the dynamic polarizability of an atom can be represented using the single-oscillator model (19). For example, for the metastable helium atom  $\text{He}^*$  we have  $\alpha(0) = 315.63$  a.u. (one a.u. of polarizability is equal to  $1.482 \times 10^{-31}$  m<sup>3</sup>),  $\omega_0 = 1.18$  eV =  $1.794 \times 10^{15}$  rad/s [42]. Equation (19) with the above value of  $\omega_0$  is appropriate in the frequency region contributing to the Casimir-Polder interaction. This was demonstrated in Ref. [8] by comparing the computational results obtained using the single-oscillator model with that using the highly accurate atomic dynamic polarizability.

Under these conditions the correction factors  $\eta(a, T)$  and  $\kappa(a, T)$  to the Casimir-Polder free energy and force, respectively, were computed in Ref. [6] using the Lifshitz formulas (5) and (7). It was shown that at short separations the effect of the nonzero skin depth of the metal wall is much greater for an atom described by the static polarizability than for an atom described by its dynamic polarizability. In particular, for a real atom characterized by the dynamic polarizability the corrections due to nonzero skin depth of a metal wall are much less than for two metal plates. For example, for two parallel plates the use of the plasma model instead of the tabulated optical data at the separations considered leads to an error of less than 2% in the free energy [39]. For atom-wall interaction, however, the use of the plasma model leads to less than 1% error in the values of the Casimir-Polder free

energy and force compared to the use of  $\varepsilon(i\xi)$  obtained from the complete tabulated optical data. One can also conclude [6] that at shorter separations a proper account of the dynamic atomic polarizability is more important than that of the nonzero skin depth. At intermediate separation distances from 1 to 3  $\mu\text{m}$  the dynamic atomic polarizability and the nonzero skin depth of the metal play qualitatively equal roles. With increasing  $a$  the role of the dynamic polarizability becomes negligible, and the free energy is determined solely by  $\alpha(0)$ . The high-temperature asymptotic expression (33) becomes applicable at  $a > 6 \mu\text{m}$ . The overall conclusion is that corrections due to nonzero skin depth, dynamic atomic polarizability and nonzero temperature should be taken into account in precise experiments. In the case of the Casimir-Polder force, the correction factors play even a stronger role than in the case of the free energy. In Sec. VI numerical computations using the Lifshitz formula (5) are performed in a wide separation region. The dielectric permittivity of wall material is found from the complex index of refraction [43]. The results are compared with the phenomenological potentials used in the theoretical description of quantum reflection.

Within the separation distance from 1 to 3  $\mu\text{m}$ , where the thermal correction is small, the role of corrections to the Casimir-Polder energy due to the nonzero skin depth and dynamic polarizability can be illustrated analytically. For this purpose one can start from the plasma and single-oscillator models and use the perturbative expansion in the relative skin depth  $\delta_0/a = \lambda_p/(2\pi a)$  and in the oscillator parameter  $\beta_A$ . Expanding the function  $h(\zeta, y)$  in Eq. (10) up to the second power in both parameters, we obtain

$$\begin{aligned}
h(\zeta, y) = & -\alpha(0)e^{-y} \left[ 2y^2 - 2\beta_A^2\zeta^2y^2 + \left( \frac{\zeta^4}{y} - 3\zeta^2y \right) \frac{\delta_0}{a} \right. \\
& \left. + \frac{1}{2} \left( 2\zeta^4 - \frac{\zeta^6}{y^2} + \zeta^2y^2 \right) \left( \frac{\delta_0}{a} \right)^2 \right].
\end{aligned} \tag{36}$$

Now we substitute (36) into the first equality of Eq. (10), change the order of integrations and calculate integrals with respect to  $\zeta$  and to  $y$ . The result is

$$E(a) = E_{\text{CP}}(a) \left[ 1 - \frac{20}{3}\beta_A^2 - \frac{8}{5} \frac{\delta_0}{a} + \frac{62}{21} \left( \frac{\delta_0}{a} \right)^2 \right], \tag{37}$$

where  $E_{\text{CP}}(a)$  is defined in Eq. (18). Substituting the above parameters for the Au wall and He\* atom, we find that at  $a = 1 \mu\text{m}$  the correction to unity due to nonzero skin depth is equal to  $-0.034$ , whereas the correction due to dynamic polarizability is equal to  $-0.046$ . At

$a = 2 \mu\text{m}$  these corrections are  $-0.018$  and  $-0.012$ , respectively, and they decrease further with the increase of separation. From Eq. (37) it can be seen that at a separation distance of about  $1 \mu\text{m}$  the corrections to the Casimir energy due to the nonzero skin depth and dynamic polarizability of the atom play a qualitatively equal role, as was discussed on the basis of the numerical computations.

The respective expression for the Casimir-Polder force is obtained as being the negative derivative of both sides of Eq. (37) with respect to  $a$

$$F(a) = F_{\text{CP}}(a) \left[ 1 - 10\beta_A^2 - 2\frac{\delta_0}{a} + \frac{31}{7} \left( \frac{\delta_0}{a} \right)^2 \right], \quad (38)$$

where  $F_{\text{CP}}(a)$  is defined in Eq. (27).

## V. ASYMPTOTIC BEHAVIOR AT LOW TEMPERATURE

We now turn our attention to the examination of the low-temperature behavior of the Casimir-Polder free energy, entropy and force for an atom interacting with a metallic wall made of real metal. This allows one to solve complicated problems on the consistency of the Lifshitz theory, as adapted for atom-wall interaction, with thermodynamics. The asymptotic expressions obtained in this section can also serve as a test for some generalizations of the Lifshitz theory. As above, we describe a real metal by means of the plasma model and the atom with a single-oscillator expression for the dynamic polarizability. Thus, separation distances larger than  $150 \text{ nm}$  are applicable.

We start once again from the function  $h(x, y)$  defined in Eq. (10) but expand it to the second power of only the parameter  $\delta_0/a$

$$\begin{aligned} h(x, y) &= -\frac{\alpha(0)}{1 + \beta_A^2 x^2} e^{-y} \left[ 2y^2 + \left( \frac{x^4}{y} - 3x^2 y \right) \frac{\delta_0}{a} \right. \\ &\quad \left. + \frac{1}{2} \left( 2x^4 - \frac{x^6}{y^2} + x^2 y^2 \right) \left( \frac{\delta_0}{a} \right)^2 \right] \\ &\equiv h_0(x, y) + h_1(x, y) + h_2(x, y), \end{aligned} \quad (39)$$

where  $h_k(x, y)$  ( $k = 0, 1, 2$ ) are the contributions to  $h(x, y)$  of order  $(\delta_0/a)^k$ . The function

$H(x)$  defined in Eq. (10) is given by

$$\begin{aligned} H(x) &= H_1(x) + H_2(x) + H_3(x), \\ H_k(x) &= \int_x^\infty dy h_k(x, y). \end{aligned} \quad (40)$$

To calculate the thermal correction to the Casimir-Polder energy defined in Eq. (10) one needs to find the difference  $H(it\tau) - H(-it\tau)$ . This is most easily done for every  $H_k(x)$  separately. Thus, for  $k = 0$

$$\begin{aligned} H_0(x) &= -\frac{2\alpha(0)}{1 + \beta_A^2 x^2} \int_x^\infty dy e^{-y} y^2 \\ &= -\frac{2\alpha(0)}{1 + \beta_A^2 x^2} e^{-x} (2 + 2x + x^2). \end{aligned} \quad (41)$$

Expanding this in powers of  $x$  we obtain

$$\begin{aligned} H_0(it\tau) - H_0(-it\tau) &= -4i\alpha(0)\tau^3 t^3 \left[ \frac{1}{3} \right. \\ &\quad \left. - \left( \frac{1}{10} - \frac{\beta_A^2}{3} \right) \tau^2 t^2 + \left( \frac{1}{168} - \frac{\beta_A^2}{10} + \frac{\beta_A^4}{3} \right) \tau^4 t^4 \right]. \end{aligned} \quad (42)$$

Substituting Eq. (42) into the third equality of Eq. (10) and integrating in  $t$ , we find the respective contribution to the thermal correction which is given by

$$\begin{aligned} \Delta_T \mathcal{F}_0(a, T) &= \frac{\hbar c \alpha(0)}{128 \pi a^4} \tau^4 \left[ \frac{1}{45} - \frac{\tau^2}{315} \left( 1 - \frac{10}{3} \beta_A^2 \right) \right. \\ &\quad \left. + \frac{\tau^4}{5040} \left( 1 - \frac{84}{5} \beta_A^2 + 56 \beta_A^4 \right) \right]. \end{aligned} \quad (43)$$

For  $\beta_A = 0$  this is just the thermal correction for an atom described by the static polarizability near an ideal metal plane calculated using a different method in Sec. III and contained in Eqs. (24) and (26).

In a similar way, for  $k = 1$  one has

$$\begin{aligned} H_1(x) &= -\frac{\alpha(0)}{1 + \beta_A^2 x^2} \frac{\delta_0}{a} \int_x^\infty dy e^{-y} \left( \frac{x^4}{y} - 3x^2 y \right) \\ &= \frac{\alpha(0)}{1 + \beta_A^2 x^2} \frac{\delta_0}{a} \left[ 3x^2 e^{-x} (1 + x) - x^4 \Gamma(0, x) \right], \end{aligned} \quad (44)$$

where  $\Gamma(z, x)$  is the incomplete gamma function. Expanding this in powers of  $x$ , we obtain

$$\begin{aligned} H_1(it\tau) - H_1(-it\tau) &= i\alpha(0)\tau^4 t^4 \frac{\delta_0}{a} \\ &\quad \times \left( \pi + \pi \beta_A^2 \tau^2 t^2 - \frac{4}{45} \tau^3 t^3 \right). \end{aligned} \quad (45)$$

The contribution from this to the thermal correction is given by

$$\begin{aligned} \Delta_T \mathcal{F}_1(a, T) &= -\frac{\hbar c \alpha(0)}{128 \pi a^4} \tau^5 \frac{\delta_0}{a} \\ &\times \left[ \frac{3 \zeta_R(5)}{\pi^4} + \beta_A^2 \tau^2 \frac{45 \zeta_R(7)}{2 \pi^6} - \frac{\tau^3}{1350} \right]. \end{aligned} \quad (46)$$

For  $k = 2$  one arrives at

$$\begin{aligned} H_2(x) &= -\frac{\alpha(0)}{2(1 + \beta_A^2 x^2)} \left( \frac{\delta_0}{a} \right)^2 \int_x^\infty dy e^{-y} \left( 2x^4 - \frac{x^6}{y^2} + x^2 y^2 \right) \\ &= -\frac{\alpha(0)}{2(1 + \beta_A^2 x^2)} \left( \frac{\delta_0}{a} \right)^2 \left[ 2x^4 e^{-x} - x^6 \Gamma(-1, x) + x^2 e^{-x} (2 + 2x + x^2) \right]. \end{aligned} \quad (47)$$

After expanding in powers of  $x$  the following equality is obtained:

$$\begin{aligned} H_2(it\tau) - H_2(-it\tau) &= \frac{i\alpha(0)}{2} \tau^5 t^5 \left( \frac{\delta_0}{a} \right)^2 \\ &\times \left[ \frac{20}{3} - \pi \tau t + \frac{2}{15} (1 + 50 \beta_A^2) \tau^2 t^2 \right]. \end{aligned} \quad (48)$$

This implies that respective contribution to the thermal correction is

$$\begin{aligned} \Delta_T \mathcal{F}_2(a, T) &= -\frac{\hbar c \alpha(0)}{128 \pi a^4} \tau^6 \left( \frac{\delta_0}{a} \right)^2 \\ &\times \left[ \frac{5}{189} - \frac{45 \zeta_R(7)}{4 \pi^6} \tau + \frac{1}{1800} (1 + 50 \beta_A^2) \tau^2 \right]. \end{aligned} \quad (49)$$

Taking together Eqs. (43), (46) and (49), we find the low-temperature asymptotic behavior of the Casimir-Polder free energy

$$\begin{aligned} \Delta_T \mathcal{F}(a, T) &= \frac{\hbar c \alpha(0)}{128 \pi a^4} \tau^4 \left\{ \frac{1}{45} - \frac{\tau^2}{315} \left( 1 - \frac{10}{3} \beta_A^2 \right) \right. \\ &+ \frac{\tau^4}{5040} \left( 1 - \frac{84}{5} \beta_A^2 + 56 \beta_A^4 \right) - \tau \frac{\delta_0}{a} \left[ \frac{3 \zeta_R(5)}{\pi^4} + \beta_A^2 \tau^2 \frac{45 \zeta_R(7)}{2 \pi^6} - \frac{\tau^3}{1350} \right] \\ &\left. - \tau^2 \left( \frac{\delta_0}{a} \right)^2 \left[ \frac{5}{189} - \frac{45 \zeta_R(7)}{4 \pi^6} \tau + \frac{1}{1800} (1 + 50 \beta_A^2) \tau^2 \right] \right\}. \end{aligned} \quad (50)$$

This expression includes the effect of both the nonzero skin depth of the metal plate and the dynamic polarizability of the atom. Several terms on the right-hand side of Eq. (50) do not contribute to the Casimir-Polder force because the quantities  $\tau/a$  and  $\tau\beta_A$  do not depend on the separation distance  $a$ . Calculating the negative derivative of Eq. (50) with respect to  $a$ , one obtains the thermal correction to the Casimir-Polder force at zero temperature (38)

$$\begin{aligned} \Delta_T F(a, T) &= \frac{\hbar c \alpha(0)}{128 \pi a^5} \tau^6 \left[ \frac{2}{315} - \frac{\tau^2}{30} \left( \frac{1}{42} - \frac{1}{5} \beta_A^2 \right) \right. \\ &\left. - 3 \tau^2 \frac{\delta_0}{a} - \tau \left( \frac{\delta_0}{a} \right)^2 \left( \frac{45 \zeta_R(7)}{4 \pi^6} - 2 \tau \right) \right]. \end{aligned} \quad (51)$$

At  $\delta_0 = \beta_A = 0$  this expression coincides with the thermal correction contained in Eqs. (27) and (29) derived for an ideal metal wall interacting with an atom characterized by the static polarizability.

Equation (50) allows the calculation of the Casimir-Polder entropy at low temperature. Calculating the negative derivative with respect to temperature of both sides of Eq. (50), we arrive at

$$S(a, T) = -\frac{k_B \alpha(0)}{32a^3} \tau^3 \left[ \frac{4}{45} - \frac{2\tau^2}{105} \left( 1 - \frac{10}{3} \beta_A^2 \right) - \tau \frac{\delta_0}{a} \frac{15\zeta_R(5)}{\pi^4} - \frac{10}{63} \tau^2 \left( \frac{\delta_0}{a} \right)^2 \right]. \quad (52)$$

As we can see, this entropy goes to zero when the temperature vanishes, implying that the Nernst heat theorem is satisfied. Although in the derivation of Eq. (52) we used the plasma model, this conclusion is valid for any other approach to the description of real metals, including the Drude model approach [28]. The point to note is that the TE reflection coefficient at zero frequency does not contribute to the Casimir-Polder atom-wall interaction. Regarding the contributions of all other Matsubara frequencies and the TM reflection coefficient at  $\xi = 0$ , different theoretical approaches to the description of a real metal in the framework of the Lifshitz theory lead to practically coincident results [26]. Thus the standard Lifshitz theory of atom-wall interaction in the case of a metal wall is thermodynamically consistent. At the same time, as seen from Eq. (52),  $S(a, T)$  at low temperature is negative. Thus, this property of the atom-wall configuration, discussed above in the case of an ideal metal wall (Sec. III), is also preserved for real metal walls. Note that the asymptotic expressions (33), (34) obtained for an atom near ideal metal wall at high temperature are valid for real metal wall as well. Nonzero skin depth does not play any role at high temperatures (large separations).

In contrast to the case of metal wall, the interaction of the atom with dielectric walls runs into problems when the dc conductivity of the wall material is included into the model of the dielectric response. Specifically, in this case the Casimir entropy calculated in the framework of the Lifshitz theory takes positive value at zero temperature, i.e., the Nernst theorem is violated [44]. Theoretical results for atom-wall interaction calculated with included small dc conductivity of a dielectric wall are shown to be experimentally inconsistent [35].



## VI. ACCURACY OF THE PHENOMENOLOGICAL POTENTIAL USED TO DESCRIBE QUANTUM REFLECTION

Practically all papers devoted to the investigation of quantum reflection (see, e.g., Refs. [16, 17, 21, 22, 45, 46, 47, 48]) use the phenomenological potential of atom-wall interaction at zero temperature to calculate the reflection amplitude. In fact, the reflection amplitude for ultra cold atoms depends critically on the shape of the potential in two asymptotic regions of small and large atom-wall separations. Specifically, it was shown [45] that the reflection amplitude depends on the dimensionless parameter

$$\rho = \frac{\sqrt{2m_a}}{\hbar} \frac{C_3}{\sqrt{C_4}}, \quad (53)$$

where  $m_a$  is the mass of an atom. In this case for  $\rho < 1$  the nonretarded interaction (13) is dominant in the quantum reflection, whereas for  $\rho > 1$  the retarded interaction (18) becomes dominant. For atoms of metastable He\* interacting with Au or Si walls considered below the parameter  $\rho$  is large and the reflection amplitude mostly depends on the Casimir-Polder potential [21, 45, 46]. The shape of the potential in the transition region between the nonretarded and retarded interactions may contribute to the reflection amplitude markedly only for atoms with increased velocity. Below we compare the phenomenological potentials used in quantum reflection with more accurate interaction energies computed using the Lifshitz formula at both zero and nonzero temperature.

The most often used phenomenological potential (interaction energy) has the form

$$E(a) = -\frac{C_4}{a^3(a+l)}, \quad (54)$$

where  $l$  is a characteristic parameter with the dimension of length that depends on the material. It is supposed that at short separations  $a \ll l$  (typically at separations of order a few nanometers),  $E(a)$  coincides with the van der Waals potential  $V_3$ , so that  $C_4 = lC_3$ . The coincidence between  $E(a)$  and the Casimir-Polder potential  $V_4$  is achieved at separations of about  $10 \mu\text{m}$  where  $l$  is negligibly small in comparison with  $a$ . At such large separations the correction factor to the Casimir-Polder energy due to nonzero skin depth and dynamic atomic polarizability is practically equal to unity.

As an example we consider the Au wall and the atom of metastable He\*. Using the value of  $\alpha(0)$  presented in Sec. IV, one obtains from Eq. (18) the magnitude of the Casimir-Polder

coefficient  $C_4^{\text{Au}} \approx 1.1 \text{ eV nm}^4 \approx 1.8 \times 10^{-55} \text{ J m}^4$ . The value of the van der Waals coefficient  $C_3$  for Au can be computed from Eq. (13). In so doing one should use the tabulated optical data for the complex index of refraction of Au [43] in order to find the values of  $\varepsilon$  along the imaginary axis, and the highly accurate data for the dynamic polarizability of He\* atom [at short separations of a few nanometers the plasma model (35) and the single-oscillator model (19) are not applicable in precise computations]. The computations (see Ref. [8] for details) lead to  $C_3^{\text{Au}} \approx 1.6 \text{ a.u.} \approx 6.4 \times 10^{-3} \text{ eV nm}^4 \approx 10.2 \times 10^{-49} \text{ J m}^4$ . From this we obtain  $l^{\text{Au}} = C_4^{\text{Au}}/C_3^{\text{Au}} \approx 172 \text{ nm}$  for the Au wall and He\* atom.

In Fig. 2(a) the phenomenological interaction energy (54) multiplied by a factor  $a^4$  is plotted as a function of separation for the case of He\* atom interacting with Au wall (the dashed line). In the same figure the solid line shows the computational results for the quantity  $a^4 E(a)$ , where the accurate interaction energy  $E(a) = \mathcal{E}(a)$  is defined in Eq. (10) in accordance with the Lifshitz formula at zero temperature. As is seen in Fig. 2(a), at short and large separations the phenomenological potential (54) almost coincides with the accurate interaction energy, as given by the Lifshitz formula. To give a better understanding of the correlation of the two potentials at separations below  $1 \mu\text{m}$ , i.e., in the most important region for the experiments on quantum reflection, in Fig. 2(b) both lines are shown in an enlarged scale. It is seen that the solid and dashed lines coincide at  $a \leq 50 \text{ nm}$ . The relative difference between the accurate and phenomenological interaction energy,

$$\delta E(a) = \frac{E_{\text{acc}}(a) - E_{\text{ph}}(a)}{E_{\text{acc}}(a)}, \quad (55)$$

is a nonmonotonous function and varies from 5.7% at  $a = 100 \text{ nm}$  to 7.9% at  $a = 1 \mu\text{m}$ . The largest values of  $\delta E$  are achieved at moderate separations, which are interesting from the experimental point of view:  $\delta E = 10.2\%$ ,  $10.4\%$  and  $10.2\%$  at separation distances  $a = 300$ ,  $400$  and  $500 \text{ nm}$ , respectively.

Now we consider the atom of metastable He\* near a high resistivity Si wall (dielectric materials are often used in the experiments on quantum reflection). In this case Eq. (18) is not applicable. The value of the Casimir-Polder coefficient  $C_4^{\text{Si}} \approx 0.75 \text{ eV nm}^4$  was computed in Ref. [22] using the Lifshitz formula. The permittivity of dielectric Si along the imaginary frequency axis with  $\varepsilon^{\text{Si}}(0) = 11.66$  was computed from the tabulated optical data and Kramers-Kronig relations [8, 43]. In a similar way the value of the van der Waals coefficient  $C_3^{\text{Si}} \approx 5.5 \times 10^{-3} \text{ eV nm}^4$  was obtained in Refs. [8, 22]. This leads to  $l^{\text{Si}} \approx 136 \text{ nm}$  for a He\*

atom near Si wall.

As an illustration, in Fig. 3(a) we plot the phenomenological interaction energy (54) multiplied by a factor  $a^4$  as a function of separation for the case of He\* atom interacting with Si wall (the dashed line). The solid line presents the computational results for the quantity  $a^4|E(a)|$  obtained using the Lifshitz formula as described above. In Fig. 3(b) the same lines are reproduced on an enlarged scale at separations below  $1 \mu\text{m}$ . As is seen in Figs. 3(a,b), at separations below 50 nm and at about  $10 \mu\text{m}$  the limiting cases of a nonrelativistic and relativistic potentials  $V_3$  and  $V_4$ , respectively, are achieved. The relative difference (55) between the accurate and phenomenological interaction energies varies from 9.4% at  $a = 100 \text{ nm}$  to 8.6% at  $a = 1 \mu\text{m}$ . However, at intermediate separations  $\delta E$  achieves the largest values which are equal to 12%, 12.5%, 12.2% and 11.6% at separations  $a = 200, 300, 400, \text{ and } 500 \text{ nm}$ , respectively. Thus, for the Au wall the phenomenological interaction energy provides a more accurate model of atom-wall interaction than for the Si wall. This is connected with the fact that the strength of atom-wall interaction for Si wall is weaker than in the case of an Au wall.

The above computations using the Lifshitz formula were performed at zero temperature. It is instructive to compare the phenomenological potential (54) with the results of more accurate computations using the Lifshitz formula at the temperature at laboratory  $T = 300 \text{ K}$ . Computations were performed by substituting the same, as above, dielectric permittivity of Au and Si and dynamic polarizability of He\* atom along the imaginary frequency axis into Eq. (5). The computational results for the quantity  $a^4|\mathcal{F}(a, T)|$  are shown by the solid lines in Fig. 4(a) for the Au wall and in Fig. 4(b) for the Si wall. In addition, in these figures the same results, as in Figs. 2(a) and 3(a), for the quantity  $a^4|E(a)|$ , where  $E(a)$  is the phenomenological potential (54) for Au and Si walls, respectively, are reproduced with dashed lines. From the comparison between Figs. 2(a) and 4(a) it is seen that for an Au wall at separations  $a \leq 2 \mu\text{m}$  from He\* atom the relative differences between the accurate and phenomenological potentials are approximately the same in the cases when the accurate potential is computed at zero temperature or at  $T = 300 \text{ K}$ . However, with the increase of separation the accurate potential, i.e., the free energy, computed at  $T = 300 \text{ K}$  (the solid line) deviates significantly from the phenomenological potential in accordance with the classical limit in Eq. (33). For Au [Fig. 4(a)] the largest deviation shown in the figure is equal to 31%. It is achieved at  $a = 5 \mu\text{m}$ .

For the  $\text{He}^*$  atom near the Si wall [Fig. 4(b)], the thermal effects play a more important role. The comparison between Figs. 3(a) and 4(b) demonstrates that here the differences between the accurate,  $\mathcal{F}(a, T)$ , and phenomenological,  $E(a)$ , potentials can be considered as temperature-independent only below  $0.5 \mu\text{m}$ . Computations show that at  $a = 1 \mu\text{m}$  the relative difference between them is equal to 9.6% (whereas, as indicated above, it is equal to only 8.6% when the zero-temperature Lifshitz formula is used). At the separation  $a = 5 \mu\text{m}$  the relative difference between the accurate temperature-dependent and phenomenological potentials achieves 43.5%.

Larger deviations between the accurate temperature-dependent potential and the phenomenological potential for dielectrics than for metals are explained by the existence of temperature and separation regions where the Casimir-Polder entropy is negative (see Secs. III–V). The phenomenon of negative entropy occurs only for atoms near a metallic plate. As a result, within some range of temperatures, the sign of the thermal correction to the Casimir-Polder energy is opposite to the sign of the energy and the respective free energy becomes nonmonotonic. This makes smaller the difference between the accurate free energy, as computed by the Lifshitz formula, and the phenomenological potential. On the contrary, for an atom near a dielectric wall the Casimir-Polder entropy is always positive [44]. This follows from the same property of the entropy in the configuration of two dielectric plates [31, 49]. Then the thermal correction and the Casimir-Polder energy have the same sign and the magnitude of the free energy is a monotonously increasing function of the temperature. Thus, with the increase of temperature (or separation) differences between the accurate free energy and the phenomenological potential can only increase.

## VII. CONCLUSIONS AND DISCUSSION

In the foregoing we have investigated some novel aspects of the Casimir-Polder interaction between an atom and a metal wall. For an ideal metal wall, the cases of short separations on the one hand, and moderate and large separations, on the other hand, were considered. At short separations, the delicate problem connected with the dependence of the Casimir-Polder free energy on the velocity of light was discussed. At moderate and large separations the analytical expressions for the Casimir-Polder free energy, force and entropy were obtained. It is shown that the Nernst heat theorem is satisfied, but at low temperatures the

Casimir-Polder entropy takes negative values. This conclusion was extended to the case of real metals. First, the role of different corrections due to nonzero skin depth, dynamic atomic polarizability and nonzero temperature was discussed and simple analytical expressions applicable to real metal walls were obtained. Then, the asymptotic behavior of the Casimir-Polder free energy and force was derived for an atom near a real metal wall. This permitted us to prove the Nernst heat theorem and demonstrates that the Casimir-Polder entropy takes negative values within some temperature range, as is the case of ideal metal wall.

The results obtained were applied to compare the phenomenological potential used in the theoretical interpretations of experiments on quantum reflection and the accurate atom-wall interaction energy computed on the basis of the Lifshitz theory. This comparison was performed for metastable  $\text{He}^*$  atoms within a wide separation region from 20 nm to  $10\ \mu\text{m}$  for both metal and dielectric walls. It was shown that at separations below  $1\ \mu\text{m}$  the phenomenological potential deviates from the accurate one up to 10.4% for a metal (Au) wall and up to 12.5% for a dielectric (Si) wall. At a separation  $a = 5\ \mu\text{m}$ , where the thermal effect plays an important role, the relative differences between the accurate and phenomenological potentials achieve 31% and 43.5% for metallic and dielectric walls, respectively. The decreased relative differences of the accurate and phenomenological potentials for metal walls are explained by the negativeness of the Casimir-Polder entropy. Bearing in mind that most of experiments on quantum reflection are performed with dielectric walls, the use of a more accurate potential seems to be preferable for the comparison of the measurement data with theory.

### Acknowledgments

V.B.B. and C.R. are grateful to CNPq, FAPESQ-PB/CNPq (PRONEX) and FAPES-ES/CNPq (PRONEX) for partial financial support. G.L.K. and V.M.M. were supported by Deutsche Forschungsgemeinschaft, Grant No 436 RUS 113/789/0–4.

- 
- [1] J. Mahanty and B. W. Ninham, *Dispersion Forces* (Academic Press, London, 1976).  
[2] J. E. Lennard-Jones, *Trans. Faraday Soc.* **28**, 333 (1932).

- [3] H. B. G. Casimir and D. Polder, *Phys. Rev.* **73**, 360 (1948).
- [4] E. M. Lifshitz, *Zh. Eksp. Teor. Fiz.* **29**, 94 (1956) [*Sov. Phys. JETP* **2**, 73 (1956)].
- [5] E. M. Lifshitz and L. P. Pitaevskii, *Statistical Physics*, Part. II (Pergamon Press, Oxford, 1980).
- [6] J. F. Babb, G. L. Klimchitskaya, and V. M. Mostepanenko, *Phys. Rev. A* **70**, 042901 (2004).
- [7] M. Antezza, L. P. Pitaevskii, and S. Stringari, *Phys. Rev. A* **70**, 053619 (2004).
- [8] A. O. Caride, G. L. Klimchitskaya, V. M. Mostepanenko, and S. I. Zanette, *Phys. Rev. A* **71**, 042901 (2005).
- [9] C. I. Sukenik, M. G. Boshier, D. Cho, V. Sandoghdar, and E. A. Hinds, *Phys. Rev. Lett.* **70**, 560 (1993).
- [10] G. Barton, *Proc. Roy. Soc. Lond. A* **410**, 141 (1987).
- [11] G. Barton, *Proc. Roy. Soc. Lond. A* **410**, 175 (1987).
- [12] V. U. Nayak, D. E. Edwards, and N. Masuhara, *Phys. Rev. Lett.* **50**, 990 (1983).
- [13] J. J. Berkhout, O. J. Luiten, I. D. Setija, T. W. Hijmans, T. Mizusaki, and J. T. M. Walraven, *Phys. Rev. Lett.* **63**, 1689 (1989).
- [14] J. M. Doyle, J. C. Sandberg, I. A. Yu, C. L. Cesar, D. Kleppner, and T. J. Greytak, *Phys. Rev. Lett.* **67**, 603 (1991).
- [15] I. A. Yu, J. M. Doyle, J. C. Sandberg, C. L. Cesar, D. Kleppner, and T. J. Greytak, *Phys. Rev. Lett.* **71**, 1589 (1993).
- [16] F. Shimizu, *Phys. Rev. Lett.* **86**, 987 (2001).
- [17] V. Druzhinina and M. DeKieviet, *Phys. Rev. Lett.* **91**, 193202 (2003).
- [18] Y. Lin, I. Teper, C. Chin, and V. Vuletić, *Phys. Rev. Lett.* **92**, 050404 (2004).
- [19] B. Segev, R. Côté, and M. G. Raizen, *Phys. Rev. A* **56**, R3350 (1997).
- [20] R. B. Doak and A. V. G. Chizmeshya, *Europhys. Lett.* **51**, 381 (2000).
- [21] H. Friedrich, G. Jacoby, and C. G. Meister, *Phys. Rev. A* **65**, 032902 (2002).
- [22] H. Oberst, Y. Tashiro, K. Shimizu, and F. Shimizu, *Phys. Rev. A* **71**, 052901 (2005).
- [23] B. Geyer, G. L. Klimchitskaya, and V. M. Mostepanenko, *Phys. Rev. A* **72**, 022111 (2005).
- [24] B. Geyer, G. L. Klimchitskaya, and V. M. Mostepanenko, *Int. J. Mod. Phys. A* **21**, 5007 (2006).
- [25] B. Geyer, G. L. Klimchitskaya, and V. M. Mostepanenko, *Ann. Phys. (N.Y.)* **323**, 291 (2008).
- [26] V. B. Bezerra, G. L. Klimchitskaya, V. M. Mostepanenko, and C. Romero, *Phys. Rev. A* **69**,

- 022119 (2004).
- [27] V. B. Bezerra, R. S. Decca, E. Fischbach, B. Geyer, G. L. Klimchitskaya, D. E. Krause, D. López, V. M. Mostepanenko, and C. Romero, *Phys. Rev. E* **73**, 028101 (2006).
- [28] J. S. Høyve, I. Brevik, J. B. Aarseth, and K. A. Milton, *J. Phys. A: Math. Gen.* **39**, 6031 (2006).
- [29] V. B. Bezerra, G. Bimonte, G. L. Klimchitskaya, V. M. Mostepanenko, and C. Romero, *Eur. Phys. J. C* **52**, 701 (2007).
- [30] F. Intravaia and C. Henkel, *J. Phys. A: Math. Theor.* **41**, 164018 (2008).
- [31] B. Geyer, G. L. Klimchitskaya, and V. M. Mostepanenko, *Phys. Rev. D* **72**, 085009 (2005).
- [32] F. Chen, G. L. Klimchitskaya, V. M. Mostepanenko, and U. Mohideen, *Optics Express* **15**, 4823 (2007).
- [33] F. Chen, G. L. Klimchitskaya, V. M. Mostepanenko, and U. Mohideen, *Phys. Rev. B* **76**, 035338 (2007).
- [34] G. L. Klimchitskaya and B. Geyer, *J. Phys. A: Math. Theor.* **41**, 164032 (2008).
- [35] G. L. Klimchitskaya and V. M. Mostepanenko, *J. Phys. A: Math. Theor.* **41**, 312002(F) (2008).
- [36] S. Y. Buhmann and D.-G. Welsch, *Progr. Quant. Electronics* **31**, 51 (2007).
- [37] S. Y. Buhmann and S. Scheel, *Phys. Rev. Lett.* **100**, 253201 (2008).
- [38] V. M. Mostepanenko and N. N. Trunov, *The Casimir Effect and its Applications* (Clarendon Press, Oxford, 1997).
- [39] M. Bordag, U. Mohideen, and V. M. Mostepanenko, *Phys. Rep.* **353**, 1 (2001).
- [40] J. Feinberg, A. Mann, and M. Revzen, *Ann. Phys. (N.Y.)* **288**, 103 (2001).
- [41] A. Scardicchio and R. L. Jaffe, *Nucl. Phys. B* **743**, 249 (2006).
- [42] R. Brühl, P. Fouquet, R. E. Grisenti, J. P. Toennies, G. C. Hegerfeldt, T. Köhler, M. Stoll, and C. Walter, *Europhys. Lett.* **59**, 357 (2002).
- [43] *Handbook of Optical Constants of Solids*, ed. E. D. Palik (Academic, New York, 1985).
- [44] G. L. Klimchitskaya, U. Mohideen, and V. M. Mostepanenko, arXiv:0802.2698; *J. Phys. A: Math. Theor.* **41**, 432001 (2008).
- [45] A. Jurisch and H. Friedrich, *Phys. Rev. A* **70**, 032711 (2004).
- [46] J. Madroñero and H. Friedrich, *Phys. Rev. A* **75**, 022902 (2007).
- [47] A. Yu. Voronin and P. Froelich, *J. Phys. B: At. Mol. Opt. Phys.* **38**, L301 (2005).
- [48] A. Yu. Voronin, P. Froelich, and B. Zygelman, *Phys. Rev. A* **72**, 062903 (2005).

- [49] G. L. Klimchitskaya, B. Geyer, and V. M. Mostepanenko, *J. Phys. A: Math. Gen.* **39**, 6495 (2006).



## Figures

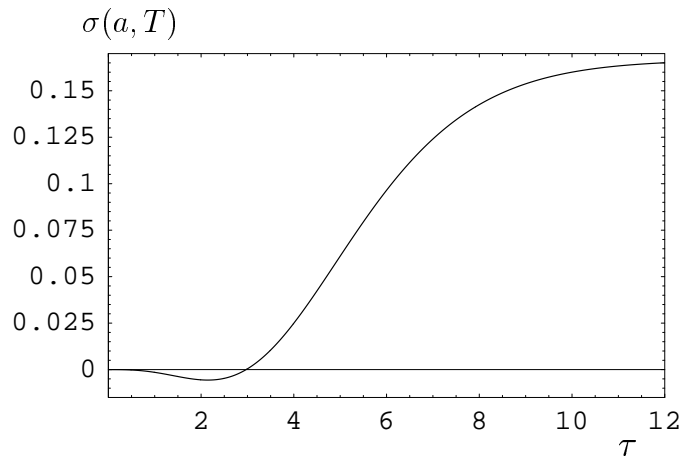


FIG. 1: The entropy factor  $\sigma$  from Eq. (30) for an atom near an ideal metal wall as a function of  $\tau$ .

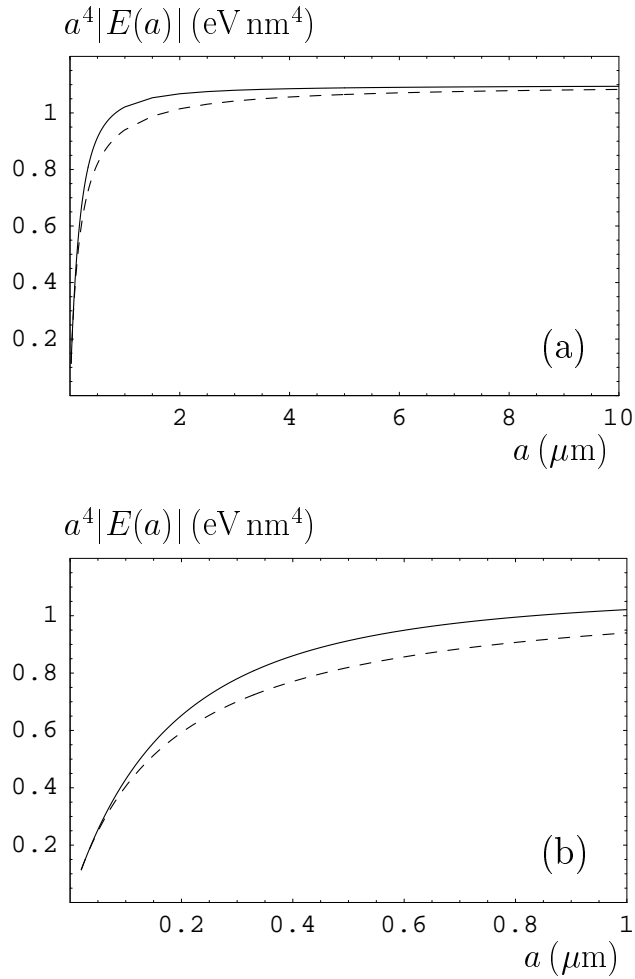


FIG. 2: Magnitude of the interaction energy between an atom of metastable  $\text{He}^*$  and Au wall multiplied by the fourth power of separation versus separation. Computations are performed using the Lifshitz formula at  $T = 0$  (the solid lines) and the phenomenological potential (54) (the dashed lines). (a) Separation varies from 20 nm to 10  $\mu\text{m}$ . (b) Separation varies from 20 nm to 1  $\mu\text{m}$ .

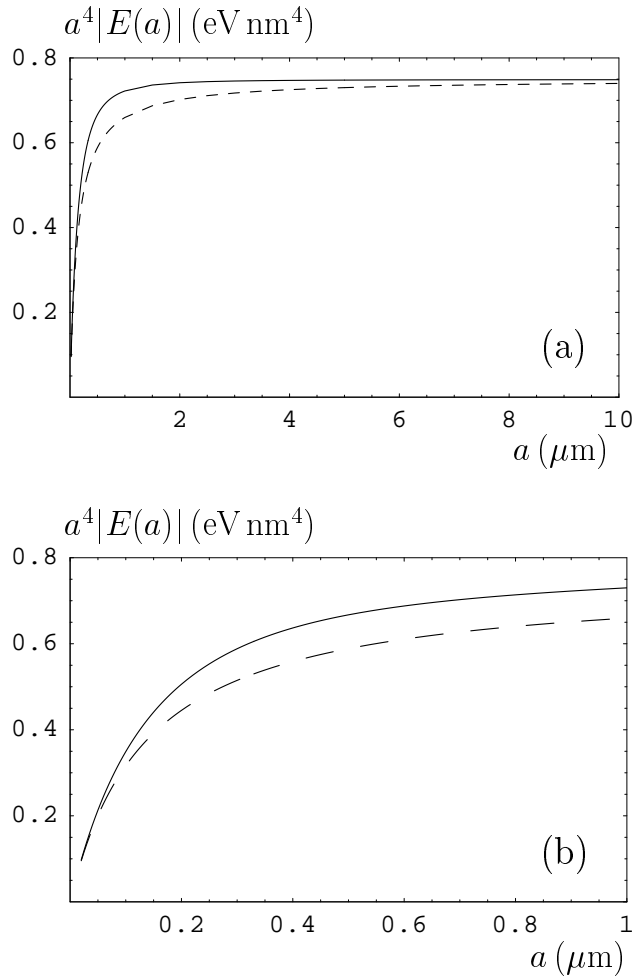


FIG. 3: Magnitude of the interaction energy between an atom of metastable  $\text{He}^*$  and Si wall multiplied by the fourth power of separation versus separation. Computations are performed using the Lifshitz formula at  $T = 0$  (the solid lines) and the phenomenological potential (54) (the dashed lines). (a) Separation varies from 20 nm to 10  $\mu\text{m}$ . (b) Separation varies from 20 nm to 1  $\mu\text{m}$ .

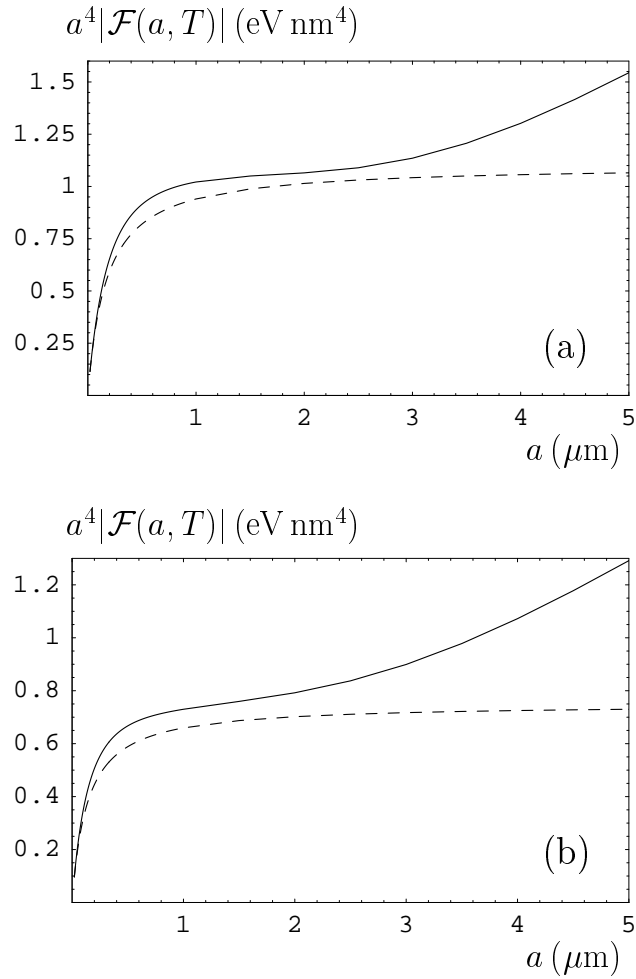


FIG. 4: Magnitude of the free energy between an atom of metastable  $\text{He}^*$  and (a) Au or (b) Si wall multiplied by the fourth power of separation as a function of separation is shown by the solid lines. The free energy is computed at  $T = 300\text{K}$  using the Lifshitz theory. For comparison the phenomenological potential (54) for (a) Au and (b) Si walls is shown by the dashed lines.